ICRC 2001

Results from the SPI imaging test setup

C. B. Wunderer[1], **P. Connell**[2], **R. Diehl**[1], **R. Georgii**[1], **J. W. Hammer**[3], **A. v. Kienlin**[1], **G. G. Lichti**[1], **F. Sanchez**[4], **V. Schönfelder**[1], **A. Strong**[1], and **G. Vedrenne**[5]

[1]MPE Garching, Germany
[2]Univ. Birmingham, U.K.
[3]IfS Univ. Stuttgart, Germany
[5]CESR Toulouse, France

Abstract. The SPI Imaging Test Setup (SPITS) was built at MPE to allow experimental verification of the imaging properties of the Spectrometer onboard INTEGRAL (SPI). Of special importance is the possibility to validate simulations - which are needed for SPI image reconstruction - with laboratory measurements.

SPITS consists of a coded mask and two Germanium detectors. The coded mask is based on a SPI mask development model, has the same Tungsten-alloy HURA mask coding as SPI, and is made of SPI flight model materials. The two hexagonal Ge-detectors in their Al caps (each 6 cm side-to-side and 7 cm long) are from the same manufacturing line as the SPI flight detectors. They are housed in a common Al end cap and cooled with liquid nitrogen. Mounted on an XY-table, they can be moved to cover the 19 Ge detector positions of the SPI camera. The SPI plastic scintillator anticoincidence is replaced by a plexiglass sheet, and no BGO anticoincidence system is used.

We have measured the response of SPITS to radioactive sources (60 keV to 1.8 MeV) at a distance of 9 m from the detector plane. We use both image deconvolution algorithms foreseen for SPI data analysis (*spiros* and *spiskymax*) for our analysis. In addition, accelerator tests are planned for May 2001. Photons from (p,γ)-reactions (up to 9 MeV) will be used to test SPITS imaging capabilites. We present our findings for the angular resolution and the point-source-location capability of SPITS as a function of energy and for different source geometries relative to the mask coding. Thus SPITS results complement the calibration performed with the flight model of SPI.

1 Introduction

ESA's INTEGRAL observatory (Winkler, 1999) consists of two main instruments, the imager IBIS and the spectrometer SPI. Optical (OMC) and x-ray (JEM-X) monitors are

Correspondence to: C. B. Wunderer (CoW@mpe.mpg.de)

added to provide multi-wavelength coverage. While IBIS is optimized for high angular resolution, SPI will deliver high-resolution spectra (2.2 keV FWHM at 1.33 MeV) with an angular resolution of 2.5^o FWHM in the energy range 20 keV - 8 MeV (Mandrou et al., 1996; Trams, 2000). All of INTEGRAL's instuments except OMC use coded masks for imaging. SPI's mask consists of 63 hexagonal opaque elements made from tungsten-alloy. Each mask element is 60 mm side-to-side and 30 mm thick, enough to absorb gamma-rays up to several MeV. SPI's position-sensitive detector is a Germanium 'camera' with 19 hexagonal pixels, each a hexagonal high purity Ge crystal 56 mm side-to-side and 70 mm long.

The technique of using coded apertures, although well established in the x-ray domain (see e.g. Badiali et al. (1985) and references therein), will be used by INTEGRAL's instruments for the first time on a space platform up to 10 MeV. Studies of the imaging capabilities of SPI were performed using GEANT and other simulation tools (Skinner et al., 1997; Connell et al., 1999; Strong et al., 1999). The SPI Imaging Test Setup was built to complement the theoretical studies of SPI imaging performance and to provide the chance to test SPI imaging algorithms long before launch.

SPITS measurements complement the SPI flight model (FM) calibrations which took place in April/May 2001. While the SPI FM calibration measurements for imaging purposes were restricted to point sources at energies below 2.5 MeV, SPITS is currently (May/June 2001) taking imaging data at the Stuttgart Dynamitron at photon energies up to 9.1 MeV and has been used to image an extended 511 keV source.

2 The SPI Imaging Test Setup

SPITS consists of two Ge detectors taken from the SPI FM manufacturing line. These two detectors are mounted in a common Al end cap. In order to measure a complete SPI image (consisting of spectra from 19 Ge detectors), the two SPITS detectors are moved on an XY-table to cover the 19 Ge

positions in 11 consecutive measurements. This is feasible since on the ground with long-lived sources neither source activity nor background conditions change significantly with time. The SPITS coded aperture was built from a SPI mask development model. The HURA code as well as all materials used are identical to those of the SPI FM mask. SPI's antico-incidence system is not necessary in the laboratory environment. Where its components influence the imaging properties for sources in the field-of-view, they have been emulated using plexiglass. A more detailed description of the test setup can be found in Wunderer et al. (2001a).

3 Image Analysis Algorithms

Analysis of SPITS data is performed using the two image deconvolution algorithms developed for SPI. The first, *spiros* (Connell et al., 2001), uses cross-correlation followed by an iterative removal-of-sources algorithm, while *spiskymax* (Strong et al., 1995) uses a maximum-entropy method to reconstruct the whole image at once. Image entropy is a measure of structure in the image. Maximizing image entropy is equivalent to determining the smoothest image consistent with the data. Most of the analysis presented here was performed using *spiskymax* only; the corresponding *spiros* analysis is to follow. While *spiros* returns the coordinates of the reconstructed sources and corresponding fluxes, *spiskymax*'s output is an image. Source fluxes can be calculated in *spiskymax* from a sky region given to the algorithm as input (we have used the true source position for this), they are determined by comparing the flux in a circular 'source region' with that in a surrounding 'background region'. We have localized sources in the *spiskymax* images by either searching for the brightest pixel of an image or by fitting a 2-D gaussian to the image and using its peak as the source position.

For image analysis, image response functions (IRFs) are required that reflect each detector's response to a source at any given point of the sky for any photon energy. For SPI imaging, these are calculated using a combination of GEANT and ray-tracing algorithms. SPITS, due to the finite distance of its sources and to differences between SPITS and SPI mass models, needs its own IRFs which were calculated using ray-tracing only. The current SPITS IRFs are calculated on a 0.2^o sky grid. Linear interpolation of the IRFs for intermediate angles is not accurate enough in some instances - as a result, *spiskymax* localization of point sources is quantized in 0.2^o steps.

4 Measurements

We have exposed SPITS to several point sources placed at 9 m from the detection plane. Using a source holder which grants easy reproducibility of source positions within a $5^o \times 9^o$ region in the field of view, we have recorded image data at 60 keV to 1.8 MeV.

Raw SPITS data consist of count spectra from each of the 19 Ge detector positions. Both imaging algorithms require
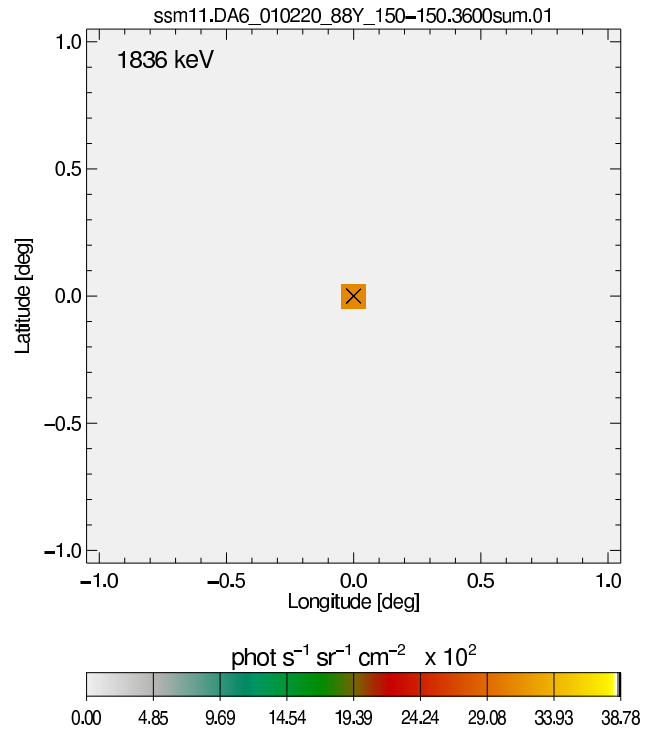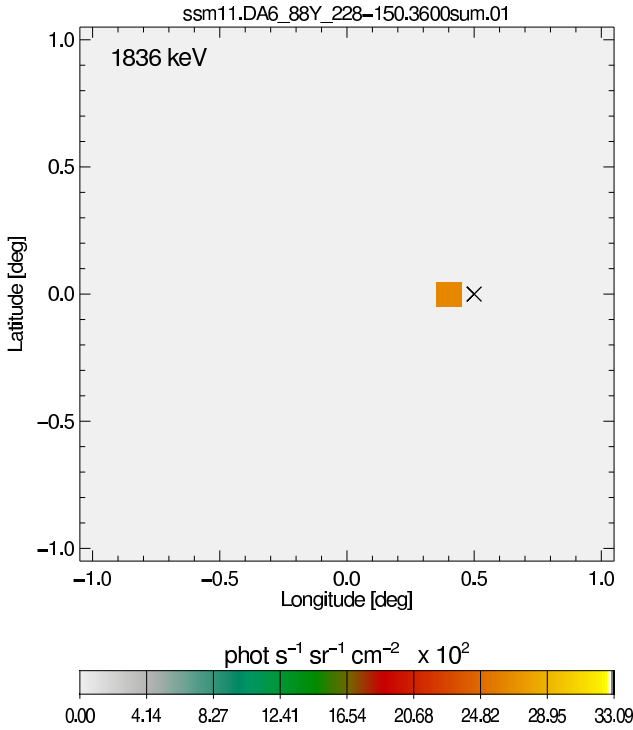

Fig. 1. ^{88}Y source at 0° - 0° reconstructed in the 1836 keV line using *spiskymax*. $\times$ denotes the true source position.

counts in an energy band (with poissonian statistics applicable) and the corresponding background estimate as input. The background estimate for SPITS data is obtained by fitting the line and underlying continuum in each spectrum and then computing the continuum counts in the region used for event binning. To determine the line counts, we use bins ± 2 σ wide.

### 4.1 SPITS Point Source Localization Accuracy

SPITS's capability to correctly locate a single point source at several positions relative to the telescope axis and at several different photon energies can be determined from these data. We observe that, for the localization of a single strong point source (using a 661 keV source at different positions), *spiros* is accurate to less than 0.15^o while *spiskymax* results differ by up to 0.25^o from the true source position. Analyzing such data at several different energies, it becomes evident that differing background continuum levels (higher at 60 keV than at 1.8 MeV) and somewhat differing source count rates cause large variations in the reconstruction accuracies. The largest localization errors observed in a large sample of 60 keV to 1.8 MeV data are 0.5^o using *spiskymax* with the (very simplistic) 'brightest pixel' approach. In the same sample, the largest error observed from spiros is on the order of 0.3^o. With improved methods of obtaining the background level and possibly using corrected (non-poissonian) line counts, we should be able to largely filter out differences arising from measurement statistics in future work. The current status of

Fig. 2. ^{88}Y source at 0.5^o - 0° reconstructed in the 1836 keV line using *spiskymax*. $\times$ denotes the true source position.

SPITS point source localization is described in more detail in Wunderer et al. (2001b). In Figures 1 and 2, we show images of an ^{88}Y source in its 1836 keV line at different angles of incidence towards SPITS. Note that while the source at 0° is reconstructed at the correct position, the source at 0.5^o is reconstructed at 0.4^o. This is caused by the IRF grid of $0.2^o \times 0.2^o$ which has an effect on *spiskymax* source reconstruction. Finer IRF grids remove this problem but were not availiable yet for the analysis presented here.
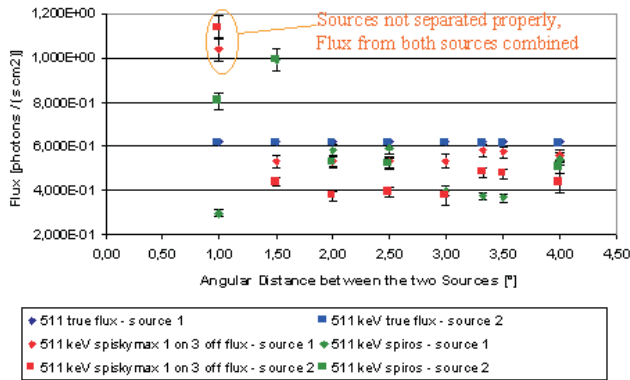
Fig. 3. True and reconstructed source fluxes for two ^{22}Na sources separated between 1° and 4°, imaged in the 511 keV line.
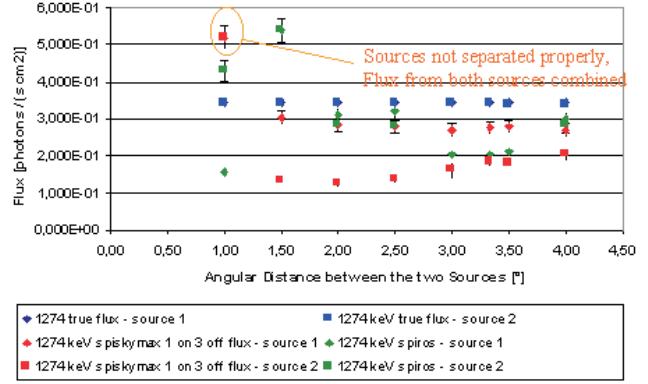
Fig. 4. True and reconstructed source fluxes for two ^{22}Na sources separated between 1° and 4°, imaged in the 1274 keV line.

## 4.2 Reconstructing Multiple Point Sources

In order to determine SPITS' capability to correctly separate and locate two close point sources of equal energy and equal intensity, we have added raw count spectra recorded with one of our calibration sources at two different positions. Thus, we obtain one dataset with two sources.

We analyze these data in the same way we analyze the single source datasets with both *spiskymax* and *spiros*. For flux determination, the methods used in the two algorithms differ, as explained above. Figures 3 and 4 show the fluxes reconstructed by both algorithms for pairs of ^{22}Na sources separated by between 1° and 4°. We have analyzed both the 511 keV and 1274 keV lines. Source fluxes from both sources should be (nearly) the same. In both energy bands and using both reconstruction algorithms, we see systematically low flux values. This may be caused either by inaccuracies in the IRFs we use, or else by problems in the reconstruction algorithms. Since both algorithms exhibit the same tendency of yielding low flux values, faults in the IRFs are probably the most likely explanation. If the IRFs are at fault, then the IRFs are based on a higher probability of a source photon interacting with the Ge detectors than is the case in reality. This could be caused e.g. by material missing in the mass models used.

Further analysis and comparison of measurements at individual Ge detector positions with full-fledged MGEANT simulations should allow us to determine if the IRFs are at fault.

4.3 Imaging an Extended 511 keV Source with SPITS

One of SPI's main tasks will be to deliver images of extended emission in the light of gamma-ray lines such as the 511 keV annihilation line or the lines from ^{26}Al, ^{60}Fe, or ^{44}Ti. All calibration measurements with SPI are performed using point sources. For SPITS, we have conceived a method to generate diffuse 511 keV emission. We use a ^{88}Y source placed 12 cm behind a lead plate. Pair production in the lead plate results in 511 keV emission from the lead. The lead disc is 38 cm in
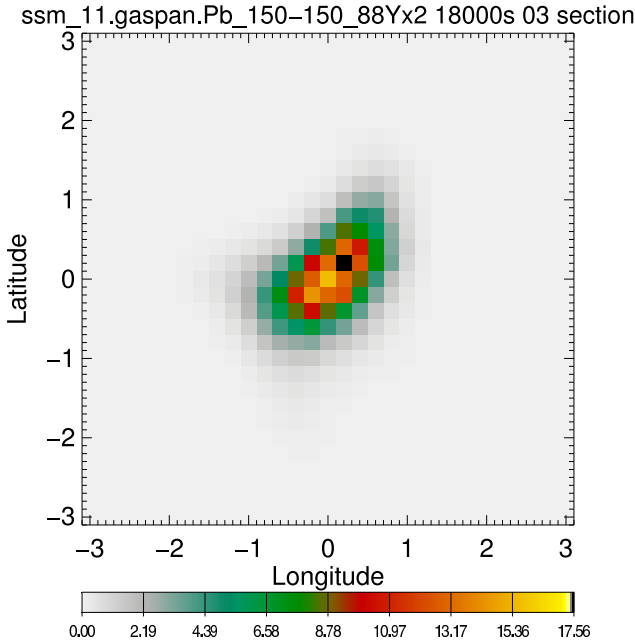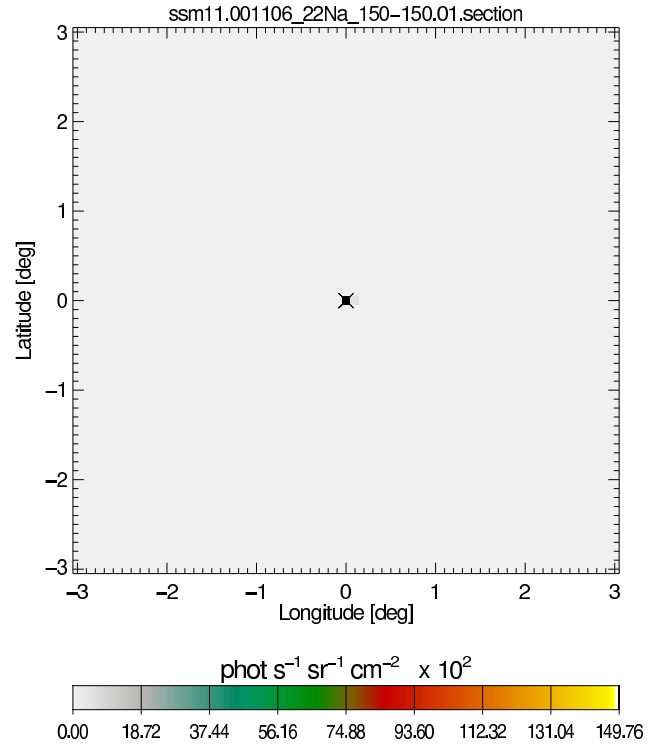
Fig. 5. Quick-look reconstruction of our 511 keV extended source using the *spiskymax* algorithm.

Fig. 6. Reconstruction of a ^{22}Na point source in the 511 keV line using the *spiskymax* algorithm.

diameter, corresponding to 2.5^o. The shape of the lead disc is optimized for maximum total 511 keV emission - i.e. the disk is thicker in the center (9 mm) and thinner at the edge (7 mm). As a result, the emission from the disk is highly non-uniform with the center of the disk yielding the highest 511 keV intensity.

We analyze the data recorded with this setup in the annihilation line using, for our first quick-look, only *spiskymax*, and obtain the image shown in Figure 5. The emission appears extended over roughly 2 degrees - this is in agreement with the actual angular size of our lead disc. A quantitative analysis of the intensity profile of the reconstructed image and comparison with the expected 511 keV emission is part of future work. We show the *spiskymax* reconstruction of a ^{22}Na point source in its 511 keV emission in Figure 6 for comparison.

5 Outlook

Currently (May/June 2001) SPITS is at the Stuttgart University's accelerator, being exposed to gamma-rays up to 9 MeV with the 'source' (i.e. the accelerator target) being placed at 0°, 0.5^o, 1°, and 3° relative to the instrument axis. Thus, we will be able to determine point source location capability and flux reconstruction accuracies over the full SPI energy range for multiple incident angles. This nicely complements the SPI flight model calibrations, which were performed with the coded aperture in place only up to 2.5 MeV. For accelerator runs at higher energies, the mask was removed to be able to determine very accurately the multi-detector response to gamma-rays up to 8 MeV (and thus, no SPI imaging data

exists above 2.5 MeV).

More detailed analysis of already existing data will be performed to reduce effects of statistics on SPITS' point source location accuracy as a function of energy. In addition, both IRFs and imaging algorithms will be checked for reasons for the systematically low reconstruction of fluxes shown above.

References

Badiali, M., et al., Astron. Astrophys. 151, 259-263, 1985.

Connell, P. H., et al., Proc. 3rd INTEGRAL Workshop 2, 397-400, 1999.

Connell, P. H., et al., Proc. 4th INTEGRAL Workshop, in press, 2001.

Mandrou, P., et al., The INTEGRAL Spectrometer SPI, Proc. 2nd INTEGRAL Workshop, 591-598, 1996.

Skinner, G. K., et al., Proc. 4th COMPTON Symposium 2, 1544-1548, 1997.

Strong, A. W., et al., Experimental Astronomy 6, 97-102, 1995.

Strong, A. W., et al., Proc. 3rd INTEGRAL Workshop 2, 221-224, 1999.

Trams, N. R., SPI Observer's Manual, INTEGRAL Science Operations Centre, INT-SOC-DOC-022, 2000.

Winkler, C., INTEGRAL - the current status, Proc. 3rd INTEGRAL Workshop, 1999.

Wunderer, C. B., et al., IEEE Trans. Nucl. Sci., accepted for publication, 2001a.

Wunderer, C. B., et al., Proc. Gamma 2001, AIP, submitted, 2001b.